Journal of Anatomy

J. Anat. (2014) **225**, pp262–269 doi: 10.1111/joa.12206

The cubital tunnel: a radiologic and histotopographic study

Veronica Macchi,[1] Cesare Tiengo,[1] Andrea Porzionato,[1] Carla Stecco,[1] Gloria Sarasin,[1] Shane Tubbs,[2] Nicola Maffulli[3] and Raffaele De Caro[1]

[1]*Department of Molecular Medicine, Institute of Anatomy, University of Padova, Padova, Italy*
[2]*Department of Cell Biology, University of Alabama at Birmingham, Birmingham, AL, USA*
[3]*Queen Mary University of London, Centre for Sports and Exercise Medicine, Mile End Hospital, London, UK*

Summary

Entrapment of the ulnar nerve at the elbow is the second most common compression neuropathy in the upper limb. The present study evaluates the anatomy of the cubital tunnel. Eighteen upper limbs were analysed in unembalmed cadavers using ultrasound examination in all cases, dissection in nine cases, and microscopic study in nine cases. In all cases, thickening of the fascia at the level of the tunnel was found at dissection. From the microscopic point of view, the ulnar nerve is a multifascicular trunk (mean area of 6.0 ± 1.5 mm^2). The roof of the cubital tunnel showed the presence of superimposed layers, corresponding to fascial, tendineous and muscular layers, giving rise to a tri-laminar structure (mean thickness 523 ± 235 μm). This multilayered tissue was hyperechoic (mean thickness 0.9 ± 0.3 mm) on ultrasound imaging. The roof of the cubital tunnel is elastic, formed by a myofascial trilaminar retinaculum. The pathological fusion of these three layers reduces gliding of the ulnar nerve during movements of the elbow joint. This may play a role in producing the symptoms typical of cubital tunnel syndrome. Independent from the surgical technique, decompression should span the ulnar nerve from the triceps brachii muscle to the flexor carpi ulnaris fascia.
Key words: anatomy; cubital tunnel; Osborne's ligament; radiological anatomy; retinaculum; ulnar nerve.

Introduction

Entrapment of the ulnar nerve at the elbow is the second most common compression neuropathy after carpal tunnel syndrome (Caliandro et al. 2012). At this level, the ulnar nerve, accompanied by the superior ulnar collateral artery, lies between the medial humeral epicondyle and the olecranon process of the ulna. It then crosses the medial collateral ligament of the elbow, and enters the flexor compartment of the forearm between the two heads of the flexor carpi ulnaris (FCU). Proximally, in the forearm, it travels between the FCU and the flexor digitorum profundus (FDP) (Moore & Dalley, 2005). In most instances, the ulnar nerve is entrapped at the level of the cubital tunnel, an elliptical fibro-osseous tunnel bordered laterally (the floor) by the capsule of the elbow joint, the posterior and transverse part of the medial collateral ligament, and the olecranon process (O'Driscoll et al. 1991; Palmer & Hughes, 2010). The cubital tunnel is bordered medially by the humeral and ulnar heads of the FCU, and anteriorly by the medial epicondyle. The roof is formed by the arcuate ligament of Osborne, which extends from the medial epicondyle to the medial aspect of the olecranon process (Siemionow et al. 2007). At this level, the structures involved in ulnar nerve compression are the aponeurosis between the two heads of the FCU (Spinner & Amadio, 2003), also called the arcuate triangular ligament or band of Osborne (Wachsmuth & Wilhelm, 1968; Wadsworth & Williams, 1977; Froimson & Zahrawi, 1980; Kleinman & Bishop, 1989), and the anconeus epitrochlearis muscle (O'Driscoll et al. 1991).

High resolution ultrasonography (Beekman et al. 2004a,b) and magnetic resonance imaging (MRI) (Bäumer et al. 2011; Ayromlou et al. 2012) can accurately assess the morphology of peripheral nerves, and have been used for imaging diagnosis of cubital tunnel syndrome. The increased cross-sectional area of the nerve at ultrasound (Scheidl et al. 2013) correlates with changes in signal intensity at MRI (Ayromlou et al. 2012). Ultrasonography also allows other features of the ulnar nerve sheath to be assessed (Beekman et al. 2004a,b), such as intraneural vascularisation (Frijlink et al. 2013), and the epineurium (Plaikner et al. 2013). Little attention has been given to the roof of the cubital tunnel

Correspondence
Raffaele De Caro, Department of Molecular Medicine, Institute of Anatomy, Via A. Gabelli 65, 35127 Padova, Italy.
T: + 39 049 8272327; F: + 39 049 8272328; E: rdecaro@unipd.it

Accepted for publication *8 May 2014*
Article published online *10 June 2014*

(Martinoli et al. 2000). Therefore, the present study evaluated the histotopographic anatomy of the ulnar nerve at the cubital tunnel, and evaluated the characteristics of the connective structures that form the roof of the entire cubital tunnel.

Materials and methods

An anatomic study was performed on 18 unembalmed cadavers (nine males, nine females; age range at death: 45–80 years) with no documented or anatomical evidence of pathology at the elbow. For each cadaver only one upper limb was studied. The study was approved by the scientific coordinator of the donation program at the University of Padova, Italy.

Radiological exams

For all 18 cases, ultrasound examination (US) was performed with an Acuvision scanner (Toshiba, Japan), equipped with a 7.5-MHz linear array transducer. All examinations were performed by the same trained operator to avoid interobserver error. During the examination, the upper limb with the dorsum of the extended wrist rested on a hard, smooth surface (Fig. 2A).

The ulnar nerve in the cubital tunnel was evaluated using cross-sectional and longitudinal scans. Cross-sectional measurements (cross-sectional area, CSA), determination of the position of the nerve in the cubital tunnel, and evaluation of the soft tissues over the ulnar nerve were all made on transverse sections. The measurements were undertaken using the software available on the ultrasound scanner.

The cadavers were then divided into two groups, one group of nine cadavers which underwent anatomical dissection, and another group of nine cadavers which underwent histotopographic study.

Dissection study

In nine cadavers (range of age: 45–72 years old at death, four males, five females), anatomical dissection was performed using 3.5× loupe magnification. A large longitudinal skin incision was made 15 cm proximally and distally from the elbow joint. Dissection was performed to reflect the skin and the subcutaneous tissues. The relation between the brachial and antebrachial fasciae with the underlying muscles and bones was analysed. The ulnar nerve was identified proximally along the medial border of the triceps brachii muscle. An opening was made in the brachial fascia 5 cm proximally to the elbow joint, and a blunt probe was inserted distally between the ulnar nerve and the fascia. Subsequently, a longitudinal incision of structures above the ulnar nerve was performed. After opening the brachial and antebrachial fasciae, the entire course of the ulnar nerve was visualised from its entrance to its exit from the cubital tunnel. The length of the ulnar nerve contained within the cubital tunnel was measured with a digital calliper (CenTech, USA) by two independent operators and the mean values of the two measurements were considered. Flexion–extension movements were performed in each phase to analyse the influence of movement on the structures overlying the nerve. In particular, with the arm immobilised by the operator, the forearm was flexed (up to to 145°), and then extended as fully as possible for five times.

Histotopographic study

A histotopographic study of the cubital tunnel was performed using nine human cadavers (age range 52–80 years old at death, five males, and four females). Full-thickness samples from 5 cm proximally to 5 cm distally to the cubital tunnel were harvested (Fig. 1A), mounted on cardboard to avoid deformation artefacts, and fixed in 10% formalin solution. For each case, 11 serial transverse samples were taken (from letters A to M) (Fig. 1B). Sections 10 μm thick were obtained from the paraffin embedded samples, and stained with haematoxylin-eosin, Azan-Mallory and Weigert-Van-Gieson stains. The microscopic examination aimed to study the characteristics of the nerve and its connective tissue envelope with particular reference to the relation between the nerve and muscular tissues. The characteristics of the epineurium and perineurium and the presence of blood vessels were analysed. All preparations were observed under a DM4500-B light microscope (Leica Microsystems, Wetzlar, Germany) and recorded in full colour (24-bit) with a digital camera (DFC 480, Leica Microsystems). Morphometric evaluation was carried out with the help of IMAGE analysis software (IMAGE J, Bethesda, MD, USA). The following parameters were recorded: thickness of the epineurium, thickness of the structures above and below the ulnar nerve, mean diameters and mean areas of the ulnar nerve trunk, mean number, and mean areas of each bundle within the ulnar nerve trunks.

Statistical analysis

Statistical analyses were carried out using ANOVA analysis and the Newman–Keuls multiple comparison test (Graphpad PRISM 3.03; Graphpad Software Inc., San Diego, CA, USA).

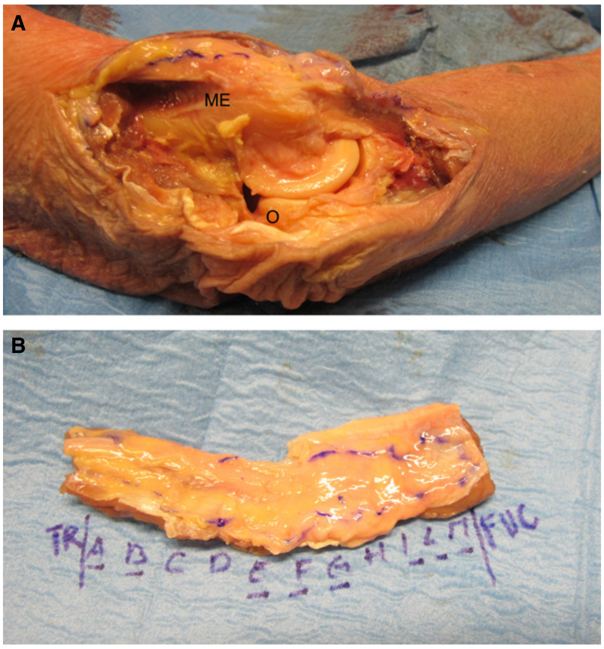

Fig. 1 (A) Sample of full, large thickness specimens from the skin to the periosteum of the cubital tunnel. (B) Subdivision into 11 serial transverse samples of the ulnar nerve (from letters A to M). ME, medial epicondyle; O, olecranon.

Results

With US, the mean CSA of the ulnar nerve within the elbow was 6.6 $\pm$ 1.2 mm^2. In all cases, the ulnar nerve in the cubital tunnel was close to the hyperechoic osseous cortex (Fig. 2A). Above the ulnar nerve, a thin hyperechoic laminar structure was identified (mean thickness 0.9 $\pm$ 0.3 mm; Fig. 2B).

In anatomical dissections, in all cases, a fibrous thickening of the brachial fascia was present at 5 cm from the joint line of the elbow, at the border between the muscle and the tendon. The thickening was formed by two laminae of fibres: the first lamina arose from the fascia of the triceps brachii muscle, with a longitudinal course in a latero-medial direction, along the axis of the limb, bridging over the elbow joint to spread into the antebrachial fascia. The second lamina of fibres appeared circumferentially, between the medial intermuscular septum and the triceps brachii muscle. Both these laminae were located over the ulnar nerve (Fig. 3A). At the level of the elbow, the longitudinal lamina was evident, whereas the circumferential lamina was poorly represented. At the level of the proximal forearm, the longitudinal component was visible, and demonstrated a fan shape on the antebrachial fascia. Moreover, another bundle of circumferential fibres was present throughout the flexor compartment. At the level of the elbow, the longitudinal lamina showed bone attachment of some of its fibres on the olecranon process and on the medial epicondyle. The probe was easily introduced through a hole in the brachial fascia and travelled along the course of the ulnar nerve. At the level of the retinaculum structure, which was intact, the pattern of the

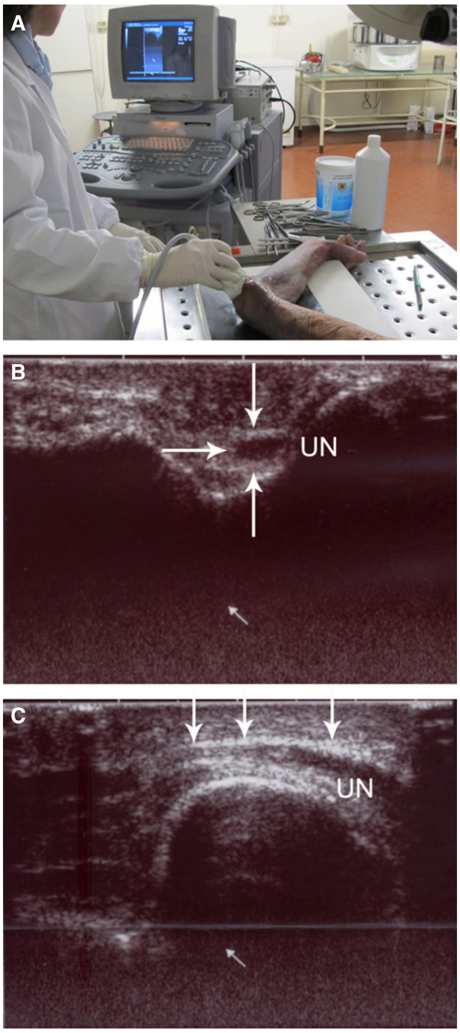

Fig. 2 (A) Location of the upper limb during the examination. (B) Transverse section of the ulnar nerve (UN). The arrows outline its periphery. c, longitudinal US section. Above the ulnar nerve, a thin hyperechoic laminar structure (arrows) is visible.

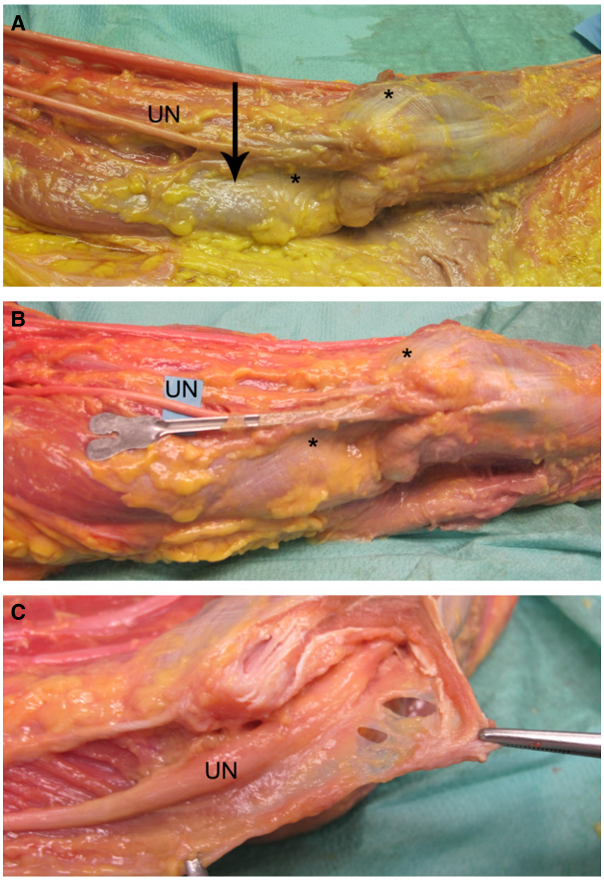

Fig. 3 (A) Two laminae of fibrous thickening are visible on the brachial fascia, one coming from the fascia of the triceps brachii muscle, with a longitudinal course (asterisk). The other lamina of fibres appeared circumferential, between the medial intermuscular septum and the triceps brachii muscle (arrow). Both of these laminae were located over the ulnar nerve. (B) A probe was introduced through a hole in the brachial fascia, and placed above the course of the ulnar nerve, with an intact retinacular structure, highlighting the pattern of the course of the fibrous laminae. (C) Incision of the brachial and antebrachial fascia, which demonstrated the absence of connective or ligament structures located between the medial epicondyle and the olecranon, above the ulnar nerve. UN, ulnar nerve.

above-described fibrous laminae was clearly recognisable (Fig. 3B). This structure adapted during movements of flexion–extension of the elbow by modifying the course of the fibrous laminae, especially the longitudinal component that became positioned more medially. After the incision of the brachial and antebrachial fascia, no connective or ligamentous structures were demonstrated between the medial epicondyle and the olecranon process above the ulnar nerve (Fig. 3C). In no case was an epitrochlear-olecranic muscle found. The mean length of the ulnar nerve in the cubital tunnel was 36 ± 15 cm. From a microscopic point of view, the ulnar nerve was a multifascicular bundle (4–18 bundles) (Fig. 4A–C), with a mean area of 6.0 ± 1.5 mm^2. Due to the small sample size, it was not possible to find statistically association between the area of the nerve and the number of fascicles, the age and the sex. The nerve was surrounded by an oval-shaped epineurium, with blood vessels located at its poles with a minimum thickness towards the bone aspect (42.3 ± 16 μm) and a maximum thickness at the poles of the oval (682.5 ± 126 μm). The perineurium was compact and thick. Above the ulnar nerve, a structure constituted of three components was evident. This structure was located between the deep adipose tissue and the ulnar nerve, and was formed from the superficial to the deep plane by the following layers: (i) a layer of loose connective tissues corresponding to the deep fascia, corresponding to a layer of loose connective tissue with undulated collagen fibre bundles with scarce elastic fibres (mean thickness 368 ± 75 μm); (ii) a layer of connective tissue corresponding to a tendineous structure (mean thickness 178 ± 83 μm); (iii) a bundle of muscle fibres (mean thickness 90 ± 26 μm). We propose to name this structure myofascial trilaminar retinaculum (Fig. 4D). The tendineous and muscular components varied in thickness along the cubital tunnel: at the level of the extremities of the tunnel, the muscular component, corresponding to the triceps brachii muscle proximally and distally to the FCU, was mainly seen. Towards the central part of the tunnel, the tendineous component was

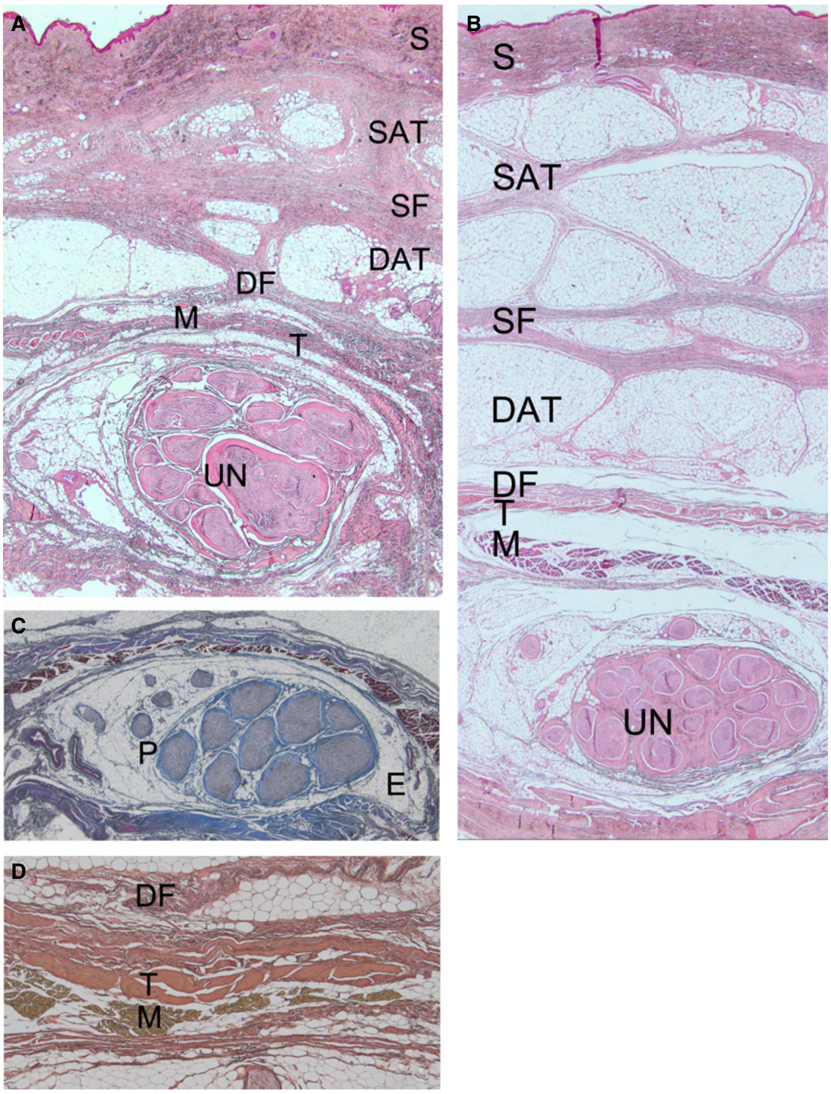

Fig. 4 The subcutaneous adipose tissue (A) at the proximal level of the cubital tunnel with poor representation of the volume of adipose lobules; (B) at the middle level of the cubital tunnel, with the adipose component more represented and thin retinacula cutis. Haematoxylin-eosin stain, Magnification, 1.25×. (C) The ulnar nerve was a multifascicular bundle (nine fascicles). The ulnar nerve was surrounded by oval-shaped epineurium (E), whereas the perineurium (P) was compact and thick. Azan–Mallory stain, magnification 1.25×. (B) Trilaminar retinacular structure above the nerve constituted by a fascial (DF), tendon (T) and muscle (M) layers. Weigert-Van-Gieson stain, magnification 25×. S, skin; SAT, superficial adipose layer; SF, superficial fascia; DAT, deep adipose layer, DF, deep fascia.

instead most prevalent. The subcutaneous adipose tissue consisted of: (i) a superficial adipose layer, in which the adipose fusiform lobules were separated by the retinacula cutis superficialis; (ii) superficial fascia; (iii) a deep adipose layer, where the lamellar adipose lobules were separated by deep retinacula cutis. The average thickness of the subcutaneous tissue was 2.8 ± 1.4 mm. At the proximal level of the cubital tunnel, the retinacular components were particularly thick, with poor representation of the volume of adipose lobules. At the middle and distal levels, the adipose component was better represented with thin retinacula cutis (Fig. 4A–B).

Discussion

The roof of the cubital tunnel is variably defined (Table 1), consisting of the triangular arcuate ligament (Wachsmuth & Wilhelm, 1968; Wadsworth & Williams, 1977; Froimson & Zahrawi, 1980; Adelaar et al. 1984; Kleinman & Bishop, 1989), or defined by the ligament of Osborne (O'Driscoll et al. 1991) or by the cubital tunnel retinaculum, a fibrous band from the medial epicondyle to the olecranon process (O'Driscoll et al. 1991). Moreover, Siemionow et al. (2007) described a fascial structure over the ulnar nerve at the level of the proximal forearm, and Karatas et al. (2009) reported fascial thickenings in the form of fibrous bands.

To our knowledge, the cubital tunnel had not been characterised microscopically. In the present study, the structural anatomy of the roof of the epitrochlear-olecranic groove shows that the ulnar nerve is covered by a three-layered myofascial retinaculum, constituted by the deep fascia, the tendon and the muscle bundles. The examined trilaminar structure has a thickness of 523 ± 235 μm, with a thickness of the fascial layer of 368 ± 75 μm, of the tendon layer of 178 ± 83 μm, and of the muscle layer of 90 ± 26 μm. James et al. (2011) reported that the thickness of the cubital tunnel retinaculum was 0.14 mm. These values of the cubital tunnel retinacula are in agreement with the value of thickness of the tendon layer of the trilaminar structure described in the present investigation. Moreover, traumatic, inflammatory or degenerative pathologies at the level of the myofascial retinaculum may cause a metaplasia of the three layers, with a prevalence of the fibrillary collagenous component and acquisition of a ligamentous appearance. The so-called ligaments described at the level of the cubital tunnel (Wachsmuth & Wilhelm, 1968; Wadsworth & Williams, 1977; Froimson & Zahrawi, 1980; Adelaar et al. 1984; Kleinman & Bishop, 1989; O'Driscoll et al. 1991) could represent the end-stage of different pathologies, which, inducing such metaplasia of the multilayered retinaculum, reduce its plasticity, causing nerve compression in place of a real ligament or accessory muscle. Also, analysis of the literature shows that the so-called ligaments were mainly found at surgery in patients with nerve compression (Table 1). During anatomical dissection one should take care not to produce undue tension on the soft tissues, which may explain the appearance of false ligaments visible during surgery.

The US study showed that a thin hyperechoic laminar structure, corresponding to the myofascial trilaminar retinaculum, is appreciable above the ulnar nerve. The mean thickness of the lamina is 0.9 ± 0.3 mm. Martinoli et al. (2000) reported that the cubital tunnel retinaculum consists of a thin fascia, visible in pathological conditions. Our study provides for the first time the normal dimensions of the cubital retinaculum: such dimensions should be confirmed in a larger sample and in pathological conditions.[1]

At ultrasound examination, the mean CSA of the ulnar nerve at the elbow was 6.6 ± 1.2 mm^2; at microscopy, the mean area was 6.0 mm^2. The ultrasonography data are in accordance with those found in the literature; at high resolution ultrasonography, the cross-sectional area ranges from 6.5 to 7.6 mm^2 (Scheidl et al. 2013). The present study did not show any evidence of a statistically significant association between the CSA of the ulnar nerve and the age and the sex of the cadavers. Other studies reported differences in the CSA of the ulnar nerve between men and women (Cartwright et al. 2007; Scheidl et al. 2013) associated only to weight, not to age, height or body mass index (Scheidl et al. 2013).

Testut (1899) and Le Double (1897) described that the roof of the cubital tunnel is reinforced by a band of transverse fibres that represents the remnants of the anconeus epitrochlearis muscle of mammals that has disappeared in humans. In fact, one of the structures implicated in ulnar nerve compression is the above muscle, whose prevalence ranges from 0% (Gonzalez et al. 2001; Karatas et al. 2009) to 11% (O'Driscoll et al. 1991). None of our specimens showed evidence of this muscle, the function of which is uncertain in humans (Testut, 1899; Von Clemens, 1957).

Regarding the anatomico-microscopic characteristics of the subcutaneous tissue, other anatomical regions are organised into layers as follows: skin (epidermis and dermis), superficial adipose tissue, horizontal fibrous layer of connective tissue (superficial fascia), deep adipose tissue, deep fascia and muscle (Lancerotto et al. 2011; Macchi et al. 2010, 2007a; Stecco et al. 2010, 2011). In the present study, we

[1]A correction was applied to the cross-sectional area measurements to account for the possible tilt of the section plane with respect to the plane perpendicular to the longitudinal axis of the nerve. To this end, the 'roundness' of each section profile was estimated (Neal & Russ, 2012) using the following equation:

$$\text{Round} = 4\text{Area}/(\pi \text{Dmax}^2)$$

Modelling the trunk of the nerve as an ideal cylinder, from basic geometrical considerations (Harris & Stocker, 1998), it follows that the parameter 'round' is simply the cosine of the angle of sectioning. Thus, the applied correction was:

$$\text{Acorr} = \text{Ameas Round}$$

Table 1 Anatomical papers that have analysed the roof of the cubital tunnel.

Authors	Number of cases	Definition	Attachment and other characteristics	Frequency%	Muscle%
Von Clemens (1957)	100 preparations	Ligamentum epitrochleo-anconeum	From medial epicondyle to the tip of the olecranon, between the two heads of FCU	70/100 70	
Osborne (1957)	Number of patients not reported	Band of fibrous tissue	Fixed attachment to medial epicondyle and a mobile one to the olecranon	100 ('every case')	
Dellon, 1986	64 cadavers 104 extremities	Osborne's ligament		77	11
O'Driscoll et al. (1991)	27 cadavers	Cubital tunnel retinaculum	Medial epicondyle to the tip of the olecranon; 4 mm wide, fusion with the FCU aponeurosis	23/27 79.3%	3/27 11
Green & Rayan, 1999	19 cadavers	Arcuate ligament	Medial epicondyle to the olecranon; continuation of the FCU aponeurosis	8/19 42.2	2/19 10.5
Matsuzaki (2001)	90 patients with cubital tunnel syndrome	Osborne's arcade		57/90 63.3	3/90 3.3
Gonzalez et al. (2001)	39 cadavers arm	Osborne's ligament	From a very thin aponeurotic structure to thickened tough ligament	39/39 100	0/39
Alp et al. (2004)	15 cadavers, 30 elbows	Cubital tunnel retinaculum and Osborne's ligament		91	
Siemionow et al. (2007)	28 cadavers	Fascia over the FDP covering the UN	Presence of 3–4 zones of fascial thickening		
Karatas et al. (2009)	6 cadavers, 12 upper limbs	Osborne's ligament	Fusion of both heads of FCU; length from medial epicondyle to olecranon 2.2 cm	1/12 8.4	0/12
James et al. (2011)	11 cadavers arm	Cubital tunnel retinaculum	From posterior and distal aspect of medial epicondyle to posteromedial aspect of olecranon; thickness 0.14 mm	9/11 81.8	1/11 9.1

Muscle: presence of anconeus epitrochlearis muscle.

have recorded, at the level of the elbow, the usual anatomic layers, with different representation of the adipose tissue along the cubital tunnel. In fact, proximally, the adipose component of the superficial and deep subcutaneous tissues is scarcely represented, with thick superficial and deep retinacula cutis. At this level, the heads of the triceps brachii muscle probably protects the ulnar nerve. At the central and distal level of the cubital tunnel, the adipose component is more evident, and could have a protective role. Moreover, the epineurium may also have a protective function, and loss of this layer may be associated with pressure palsies seen in wasted, bedridden patients (Standring et al. 2008). Macchi et al. (2007b) ascribed the low frequency of entrapment syndrome of the musculocutaneous nerve to the arrangement of its epineurium, which, thanks to the uneven disposition of the adipose tissue, may allow compliance between variations of length of the coracobrachialis muscle and the constant course of the nerve. Our microscopic study found that the epineurium surrounding the ulnar nerve is composed of multilayered concentrically arranged laminae of connective tissue with a constant arrangement along the cubital tunnel. It shows an oval-shaped morphology, with blood vessels located at its poles, with minimum thickness on the bone aspect and maximum thickness at the poles. This particular disposition could explain the nerve compression during elbow flexion attributed to the reduction of the volume of the cubital tunnel (Feindel & Stratford, 1958; Wachsmuth & Wilhelm, 1968; Apfelberg & Larson, 1973; Wadsworth & Williams, 1977), maximally evident at 135° of elbow flexion (James et al. 2011). These findings correlate well with paralysis of the ulnar nerve in people who sleep with flexed elbows (Adelaar et al. 1984).

Ulnar nerve compression at the elbow can be accomplished using open or endoscopic approaches (Wadsworth, 1977; Dellon, 1986, 1989; Zlowodzki et al. 2007; Giladi et al.

2013). In both instances, only a partial visualisation of the entire elbow fascial plane is obtained. This could lead the surgeon to identify the anomalous ligamentous structures that actually are the fibrotic degeneration of the three fascial layer of the cubital region.

After surgical decompression, in patients with chronic subluxation of the nerve (Maffulli, 2002; Capasso et al. 1998.), anterior transposition and fixation under or above the epicondylar muscles can be performed. In any case, surgical decompression of the ulnar nerve must provide extensive freeing of the multilayered retinaculum from the triceps brachii muscle fascia to the aponeurosis of the flexor carpi ulnaris.

When decompressing the cubital tunnel, we suggest performing a paramedian fascial incision along the bony lateral walls of the tunnel to maintain the roof of the tunnel in place, given its protective function. In this way, fascial scarring over the course of the ulnar nerve could be prevented.

Acknowledgements

The authors are grateful to Drs A. Cappellari and M. Corradin for skilful assistance, to Dr D. Guidolin for technical support, and to Dr G. Andretta for review of the English. We declare that we have no conflict of interest.

Author contributions

V.M. contributed to the concept and design of the manuscript, performed the ultrasound examination, and performed data analysis and interpretation. C.T. and C.S. performed the dissections and the collection of the specimens. A.P. performed analysis of the microscopic specimens and performed data analysis and interpretation. G.S. performed the morphometric analysis. S.T. and N.M contributed to critical revision of the manuscript. R.D.C. contributed to the drafting and critical revision of the manuscript.

References

Adelaar RS, Foster WC, McDowell C (1984) The treatment of the cubital tunnel syndrome. *J Hand Surg Am* **9A**, 90–95.

Alp M, Akkin SM, Yalçin L, et al. (2004) Cubital tunnel release with two limited incisions: a cadaver study. *Surg Radiol Anat* **26**, 259–262.

Apfelberg DB, Larson SJ (1973) Dynamic anatomy of the ulnar nerve at the elbow. *Plast Reconstr Surg* **51**, 79–81.

Ayromlou H, Tarzamni MK, Daghighi MH, et al. (2012) Diagnostic value of ultrasonography and magnetic resonance imaging in ulnar neuropathy at the elbow. *ISRN Neurol*, **2012**, 491892.

Bäumer P, Dombert T, Staub F, et al. (2011) Ulnar neuropathy at the elbow: MR neurography – nerve T2 signal increase and caliber. *Radiology* **260**, 199–206.

Beekman R, Schoemaker MC, Van Der Plas JP, et al. (2004a) Diagnostic value of high-resolution sonography in ulnar neuropathy at the elbow. *Neurology* **62**, 767–773.

Beekman R, Van Der Plas JP, Uitdehaag BM, et al. (2004b) Clinical, electrodiagnostic, and sonographic studies in ulnar neuropathy at the elbow. *Muscle Nerve* **30**, 202–208.

Caliandro P, La Torre G, Padua R, et al. (2012) Treatment for ulnar neuropathy at the elbow. *Cochrane Database Syst Rev* **7**, CD006839.

Capasso G, Testa V, Cappabianca S, et al. (1998) Recurrent dislocation of the ulnar nerve in athletes: a report of two cases. *Clin J Sport Med* **8**, 56–58.

Cartwright MS, Shin HW, Passmore LV, et al. (2007) Ultrasonographic findings of the normal ulnar nerve in adults. *Arch Phys Med Rehab* **88**, 394–396.

Dellon AL (1986) Musculotendinous variations about the medial humeral epicondyle. *J Hand Surg Br* **11**, 175–181.

Dellon AL (1989) Review of treatment results for ulnar nerve compression at the elbow. *J Hand Surg* **14**, 668–700.

Feindel W, Stratford J (1958) Cubital tunnel compression in tardy ulnar palsy. *Can Med Assoc J* **78**, 351–353.

Frijlink DW, Brekelmans GJ, Visser LH (2013) Increased nerve vascularization detected by color Doppler sonography in patients with ulnar neuropathy at the elbow indicates axonal damage. *Muscle Nerve* **47**, 188–193.

Froimson AI, Zahrawi F (1980) Treatment of compression neuropathy of the ulnar nerve at the elbow by epicondylectomy and neurolysis. *J Hand Surg Am* **5**, 391–395.

Giladi AM, Gaston RG, Haase SC, et al., Surgery of the Ulnar Nerve Study Group (2013) Trend of recovery after simple decompression for treatment of ulnar neuropathy at the elbow. *Plast Reconstr Surg* **131**,563e–573e.

Gonzalez MH, Lotfi P, Bendre A, et al. (2001) The ulnar nerve at the elbow and its local branching: an anatomic study. *J Hand Surg Br* **26**, 142–144.

Green JR Jr, Rayan GM (1999) The cubital tunnel: anatomic, histologic, and biomechanical study. *J Shoulder Elbow Surg* **8**, 466–470.

Harris JW, Stocker H (1998) *Handbook of Mathematics and Computational Science*. New York: Springer-Verlag.

James J, Sutton LG, Werner FW, et al. (2011) Morphology of the cubital tunnel: an anatomical and biomechanical study with implications for treatment of ulnar nerve compression. *J Hand Surg Am* **36**, 1988–1995.

Karatas A, Apaydin N, Uz A, et al. (2009) Regional anatomic structures of the elbow that may potentially compress the ulnar nerve. *J Shoulder Elbow Surg* **18**, 627–631.

Kleinman WB, Bishop AT (1989) Anterior intramuscular transposition of the ulnar nerve. *J Hand Surg Am* **14**, 972–979.

Lancerotto L, Stecco C, Macchi V, et al. (2011) Layers of the abdominal wall: anatomical investigation of subcutaneous tissue and superficial fascia. *Surg Radiol Anat* **33**, 835–842.

Le Double F (1897) *Traité Des Variations Du Systéme Musculaire de l'Homme et de Leur Signification au Point de Vue de l'Anthropologie Zoologique, I et II*. Paris: Librairie C. Reinwald.

Macchi V, Tiengo C, Porzionato A, et al. (2007a) Anatomo-radiological study of the superficial musculo-aponeurotic system of the face. *Ital J Anat Embryol* **112**, 247–253.

Macchi V, Tiengo C, Porzionato A, et al. (2007b) Musculocutaneous nerve: histotopographic study and clinical implications. *Clin Anat* **20**, 400–406.

Macchi V, Tiengo C, Porzionato A, et al. (2010) Histotopographic study of the fibroadipose connective cheek system. *Cells Tissues Organs* **191**, 47–56.

Maffulli N (2002) US in the diagnosis of ulnar nerve dislocation. *Radiology* **223**, 877–878.

Martinoli C, Bianchi S, Gandolfo N, et al. (2000) US of nerve entrapments in osteofibrous tunnels of the upper and lower limbs. *Radiographics* **20**, S199–S213.

Matsuzaki A (2001) Membranous tissue under the flexor carpi ulnaris muscle as a cause of cubital tunnel syndrome. *Hand Surg* **6**, 191–197.

Moore KL, Dalley AF (2005) *Clinically Oriented Anatomy*. 5th edn, pp. 745–748, Philadelphia: Lippincott Williams and Wilkins.

Neal FB, Russ JC (2012) *Measuring Shape*. Boca Raton: CRC Press.

O'Driscoll SW, Horii E, Carmichael SW, et al. (1991) The cubital tunnel and ulnar neuropathy. *J Bone Joint Surg (Br)* **73**, 613–617.

Osborne G (1970) Compression neuritis of the ulnar nerve at the elbow. *Hand* **2**, 10–13.

Palmer AB, Hughes TB (2010) Cubital tunnel syndrome. *J Hand Surg (Am)* **35**, 153–163.

Plaikner M, Loizides A, Loescher W, et al. (2013) Thickened hyperechoic outer epineurium, a sonographic sign suggesting snapping ulnar nerve syndrome? *Ultraschall Med* **34**, 58–63.

Scheidl E, Böhm J, Farbaky Z, et al. (2013) Ultrasonography of ulnar neuropathy at the elbow: axonal involvement leads to greater nerve swelling than demyelinating nerve lesion. *Clin Neurophysiol* **124**, 619–625.

Siemionow M, Agaoglu G, Hoffmann R (2007) Anatomic characteristics of a fascia and its bands overlying the ulnar nerve in the proximal forearm: a cadaver study. *J Hand Surg Eur* **32**, 302–307.

Spinner RJ, Amadio PC (2003) Compressive neuropathies of the upper extremity. *Clin Plast Surg* **30**, 155–173.

Standring S, Borley NR, Collins P, et al. (eds) (2008) *Gray's Anatomy*. 40th edn, p. 235. London: Churchill Livingstone.

Stecco C, Macchi V, Porzionato A, et al. (2010) The ankle retinacula: morphological evidence of the proprioceptive role of the fascial system. *Cells Tissues Organs* **192**, 200–210.

Stecco C, Macchi V, Porzionato A, et al. (2011) The fascia: the forgotten structure. *Ital J Anat Embryol* **116**, 127–138.

Testut L (1899) *Traité d'Anatomie Humaine*, p. 229, Paris: Doin, 1st tome.

Von Clemens HJ (1957) Zur morphologie des ligamentum epitrochleo-anconeum. *Anat Anz* **104**, 343–344.

Wachsmuth W, Wilhelm A (1968) Der musculus epitrochleoanconaeus und seine klinische bedeutung. *Mschr Unfallheik* **71**, 21–22.

Wadsworth TG (1977) The external compression syndrome of the ulnar nerve at the cubital tunnel. *Clin Orthop Relat Res* **124**, 189–204.

Wadsworth TG, Williams RM (1977) The cubital tunnel external compression syndrome. *Nurs Times* **73**, 1357–1359.

Zlowodzki M, Chan S, Bhandari M, et al. (2007) Anterior transposition versus simple decompression for the treatment of cubital tunnel syndrome. A meta-analysis of randomized, controlled trials. *J Bone Joint Surg (Am)* **89**, 2591–2598.